Ultra-bright, ultra-broadband hard x-ray driven by laser-produced energetic electron beams

Yin Shi, Baifei Shen, Xiaomei Zhang, Wenpeng Wang, Liangliang Ji, Lingang Zhang, Jiancai Xu, Yahong Yu, Xueyan Zhao, Xiaofeng Wang, Longqing Yi, Tongjun Xu, and Zhizhan Xu

Citation: Physics of Plasmas **20**, 093102 (2013); doi: 10.1063/1.4820777
View online: http://dx.doi.org/10.1063/1.4820777
View Table of Contents: http://scitation.aip.org/content/aip/journal/pop/20/9?ver=pdfcov
Published by the AIP Publishing

Ultra-bright, ultra-broadband hard x-ray driven by laser-produced energetic electron beams

Yin Shi, Baifei Shen,[a] Xiaomei Zhang, Wenpeng Wang, Liangliang Ji, Lingang Zhang, Jiancai Xu, Yahong Yu, Xueyan Zhao, Xiaofeng Wang, Longqing Yi, Tongjun Xu, and Zhizhan Xu

State Key Laboratory of High Field Laser Physics, Shanghai Institute of Optics and Fine Mechanics, Chinese Academy of Sciences, P.O. Box 800-211, Shanghai 201800, China

(Received 29 May 2013; accepted 13 August 2013; published online 9 September 2013)

We propose a new method of obtaining a compact ultra-bright, ultra-broadband hard X-ray source. This X-ray source has a high peak brightness in the order of 10^{22} photons/(s mm^2 mrad^2 0.1\%BW), an ultrashort duration (10 fs), and a broadband spectrum (flat distribution from 0.1 MeV to 4 MeV), and thus has wide-ranging potential applications, such as in ultrafast Laue diffraction experiments. In our scheme, laser-plasma accelerators (LPAs) provide driven electron beams. A foil target is placed oblique to the beam direction so that the target normal sheath field (TNSF) is used to provide a bending force. Using this TNSF-kick scheme, we can fully utilize the advantages of current LPAs, including their high charge, high energy, and low emittance. © *2013 AIP Publishing LLC*. [http://dx.doi.org/10.1063/1.4820777]

I. INTRODUCTION

High-energy photons with high brightness and short pulse duration from affordable tabletop systems have wide-ranging applications,[1] including biomedical imaging,[2] time-resolved molecular dynamics,[3] and non-destructive material inspection.[4]

Driven by electron beams from conventional accelerators, current X-ray sources such as synchrotron, X-ray free electron laser (XFEL), Bremsstrahlung, and Thomson scattering provide lights with different spectra, brightness, or coherence.[1,5] For example, as one of the four largest synchrotron radiation facilities, SPring-8 uses an 8 GeV electron beam to produce synchrotron radiation with energies ranging from soft X-ray (300 eV) to hard X-ray (300 keV).[1] The peak brightness at 100 keV can reach the order of 10^{24} photons/(s mm^2 mrad^2 0.1\%BW) but drops to 10^{20} photons/(s mm^2 mrad^2 0.1\%BW) at 300 keV.[1] To extend the photon energy to MeV, electron beams of higher energy are needed because of the limits of magnitude (order of 1 T) and period (order of 1 cm) of the bending magnetic field for synchrotron and free electron laser. Compton backscattering is another approach to obtain hard X-ray. The required energy of the driven electron beams in Compton backscattering is not very high according to the double Doppler shift $\hbar\omega_x = 4\gamma^2\hbar\omega_0$. For example, the electron energy is approximately 205 MeV to obtain 1 MeV hard X-ray using an 800 nm laser pulse. Given that the radiation angle is proportional to $1/\gamma$ (where γ is the relativistic factor of the electron) and if normalized emittance of the electron beam is maintained for different beam energies, an electron beam of low energy used for Compton backscattering may result in large radiation angle and low brightness. Recently, Chen *et al.* proved experimentally a MeV-energy X-ray source with a peak brightness of 10^{19} photons/(s mm^2 mrad^2 0.1\%BW) using Compton backscattering with laser-wakefield accelerated electrons.[6] Meanwhile, the betatron radiation brightness in a bubble can reach the order of 10^{23} photons/(s mm^2 mrad^2 0.1\%BW) in spectra between 20 and 150 KeV and drops nearly two orders in spectra between 1 and 7 MeV.[7]

This study proposed a new scheme of generating an ultra-brightness, ultra-broadband hard X-ray source that uses a target normal sheath field (TNSF) as the bending field. We call this scheme TNSF kick. Considering that the bending field is static, the low emittance and small radiation angle $1/\gamma$ can be exploited using highly energetic beams. TNSF is an ultra-intense electrostatic field (can reach the order 10^{12} V/m) created by space charge separation when an intense laser pulse drives the hot electrons to the rear surface of the target foil, which is usually used to accelerate protons.[8,9] The photon energy can be easily extended to the range of hard X-ray or even gamma-ray because this field is much stronger than the conventional magnetic field used for synchrotron and XFEL. Although TNSF is always perpendicular to the foil plane, the target foil in our scheme is placed oblique to the beam direction (Fig. 1) to provide a transverse static ultra-intense bending force to the electron beams and to give a powerful kick. Based on the combination of low divergence, broadband spectrum of radiation for a single energetic electron, and low emittance of a femtosecond (fs) electron beam, the TNSF kick can radiate an fs hard X-ray pulse with high peak brightness and broadband spectrum. This source may have wide-ranging applications. For example, ultrafast Laue diffraction experiments may exploit the broadband X-ray spectrum.[10] Broadband X-ray beam diffraction patterns are sensitive to microstructure.[4] Maaß *et al.*[11] demonstrated the detailed dynamics of deforming micropillars using real-time resolved white-beam Laue microdiffraction.

The electron beams used in our scheme can be produced by laser-plasma accelerators (LPAs). This method can be a tabletop X-ray source. Current LPAs can provide a beam

[a]Electronic mail: bfshen@mail.shcnc.ac.cn.

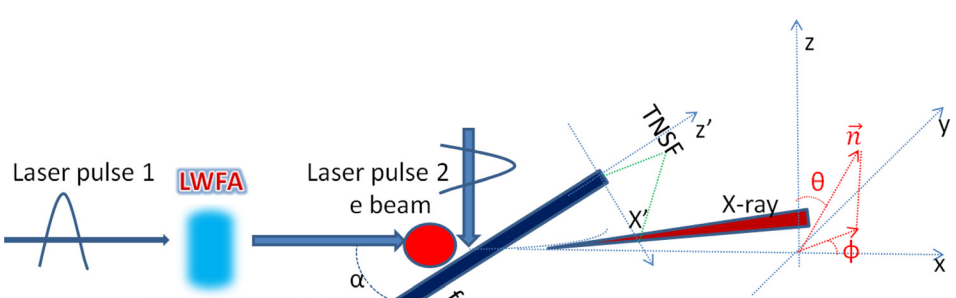

FIG. 1. Schematic of TNSF-kick X-ray source. Laser pulse 1 drives a laser wakefield acceleration to provide a high-energy electron beam, and laser pulse 2 drives a TNSF to transversely kick the electron beam. The observed plane is in the far field, where X-ray spectra are calculated.

with energy greater than 2 GeV.[12] For these electron beams, the divergence angle is only few milliradians, source size is few micrometers. The normalized emittance is comparable to that obtained in conventional high-brightness linacs.[13] However, the energy spread of beams from LPAs is still too large for many applications, such as XFEL and other monoenergetic X-ray beam sources. This large energy spread is not a disadvantage to our scheme because we want to produce a flat, ultra-broadband X-ray spectrum. Various kinds of high-brightness and compact ultrashort X-ray sources based on an LPA beam have been studied both experimentally and theoretically. Such sources include Compton backscattering,[10,14,15] synchrotron radiation,[16,17] betatron radiation,[7,18] XFEL,[19] and Bremsstrahlung radiation.[20] These sources all have their advantages and disadvantages.

The succeeding discussions take as an example a currently available LPA electron beam of high charge (320 pC), high energy spread (expanding from 0.85 GeV to 1.15 GeV), and low normalized emittance (π mm mrad). We show that an intense fs broadband X-ray with brightness in the order of 10^{22} photons/(s mm^2 mrad^2 0.1\%BW) and a flat band from 0.1 MeV to 4 MeV can be determined.

II. TRAJECTORY AND RADIATION OF SINGLE ELECTRON

First, we calculate the trajectory of a single energetic electron propagating through a supposed TNSF model, the radiation spectrum of this electron. In our scheme (Fig. 1), laser pulse 1 drives a laser wakefield acceleration to provide an energetic electron beam, and laser pulse 2 drives a TNSF to transversely kick the electron beam. The observed plane is in the far field, where X-ray spectra are calculated. To understand the electron trajectory and its radiation spectrum, a simple TNSF model is used (inset of Fig. 2), where $E_m = 1.0\times10^{12}$ V/m, $x_2 = 1.0\times10^{-6}$m, and $x_1 = 0.1x_2$. To show that these parameters are reasonable, Fig. 2 presents a two-dimensional (2D) particle-in-cell (PIC) simulation result. The laser pulse parameters in the simulation are as follows: pulse duration, 26.7 fs (FWHM); transverse diameter, 8 μm; laser wavelength, 0.8 μm; and peak normalized amplitude of the vector potential, $a=2.2$, which corresponds to an intensity of 1.0×10^{19} W/cm^2. The plasma density is set to 5 n_c (n_c is the critical density) and the foil thickness is 0.8 μm.

The equations of electron movement in the aforementioned TNSF model are as follows:

$$\begin{cases} \mathrm{d}(\gamma\beta_x)/\mathrm{d}t = -(e/mc)E(x')\sin\alpha, \\ \mathrm{d}(\gamma\beta_z)/\mathrm{d}t = (e/mc)E(x')\cos\alpha. \end{cases} \tag{1}$$

The E field is shown in the inset of Fig. 2. The solution of the previously mentioned equations can be written as

$$\begin{cases} (\gamma\beta_x)_t = (\gamma\beta_x)_0 - p_m f(t)\sin\alpha, \\ (\gamma\beta_z)_t = p_m f(t)\cos\alpha, \end{cases} \tag{2}$$

where $p_m = eE_m/mc$, $T_i = x_i/(c\sin\alpha)$ (i = 1, 2), and

$$f(t) = \begin{cases} t^2/2T_1, & 0 < t < T_1, \\ (1+T_1/T_2)t - t^2/2T_2 - (T_1/2 + T_1^2/2T_2), & T_1 < t < T_1 + T_2. \end{cases} \tag{3}$$

Based on Eqs. (2) and (3), the electron trajectory can be calculated. As an approximation, we provide the expressions of velocity under a small deviation relative to a purely numerical solution,

$$\begin{cases} \beta_x(t) \approx 1 - [1 + (p_m f(t)\cos\alpha)^2]/2\gamma_0^2, \\ \beta_z(t) \approx (p_m/\gamma_0) f(t)\cos\alpha. \end{cases} \tag{4}$$

The approximation can be used in spectrum calculation mainly because the trajectory is sufficiently smooth within the entire kick process in this study.[21] Spectrum calculations based on pure numerical trajectory are also carried out to prove the accuracy of the approximation.

For extremely high photon energies and radiation from a beam, spectrum calculations may be costly if the Lienard-Wiechert potentials are directly integrated numerically,[22]

$$\frac{\mathrm{d}^2 I}{\mathrm{d}\omega\mathrm{d}\Omega} = \frac{e^2\omega^2}{4\pi^2 c}\left|\int_{-\infty}^{\infty} \vec{n}\times(\vec{n}\times\vec{\beta}) e^{i\omega(t-\vec{n}\cdot\vec{r}(t)/c)}\mathrm{d}t\right|^2. \tag{5}$$

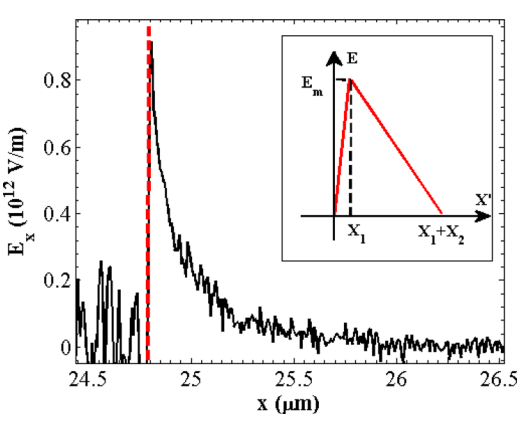

FIG. 2. 2D PIC simulation result of TNSF for a laser pulse of normalized vector potential $a = 2.2$ and plasma density $n_e = 5n_c$. Red dotted lines represent the back of the foil. The inset shows a TNSF model of $E_m = 1.0 \times 10^{12}$ V/m, $x_2 = 1.0 \times 10^{-6}$m, and $x_1 = 0.1x_2$.

This study uses a mixed analytic and numerical method as proposed by Thomas *et al.*[23] to calculate the radiation spectrum. The endpoint effects are properly included.[21]

We use an electron of energy 1 GeV and an incident angle $\alpha = \pi/18$ as an example. Fig. 3 shows the angularly resolved spectra of a single electron in the lines that are parallel and perpendicular to the plane of electron motion. As shown in the figure, the radiation spectra of the single electron are of a broad frequency band, very different from the spectra of the periodic trajectory in conventional undulator and Compton backscattering. This difference is partly due to the non-coherent superposition during half oscillation in the TNSF kick instead of periodic oscillations in the undulator,[22] leading to a continuous spectrum. On the other hand, the spectrum is expanded to a high critical frequency because of the strong TNSF. The broadband spectrum of the TNSF kick approach is similar to wiggler and synchrotron radiation. Regarding Compton scattering, radiation energy is mainly concentrated on the first several odd harmonics of the laser frequency according to the double Doppler shift formula in nonlinear Compton backscattering theory.[24] The broadband characteristic in the TNSF kick provides an ultra-broadband hard X-ray source, which will be presented later. Fig. 4 clearly shows the solid angle distribution of photons with different energies. In this figure, the radiation energy is mainly concentrated in a small solid angle $\theta \sim (-3.2, 0)$ mrad and $\phi \sim (-0.7, 0.7)$ mrad for a wide range of photon energy because of the high energy of electrons. We perform calculations for the electric field of a steep rising edge close to the PIC result. This steep rising edge minimally contributes to radiation because of the limited radiation time (not shown).

Similar to the undulator and wiggler, the dimensionless parameter $K = \gamma_0\psi$ can be defined for the TNSF kick.[22,25] Here, ψ is the maximum angle of the trajectory and γ_0 is the initial relativistic factor of the electron. The angle can be explicitly derived from the trajectory $\psi = (e/2mc^2)(x_1 + x_2)E_m \cot\alpha/\gamma_0$. In our case, $E_m = 1.0 \times 10^{12}$V/m, $x_2 = 1.0 \times 10^{-6}$m, $x_1 = 0.1x_2$, $\alpha = \pi/18$, and $\gamma_0 = 1957$, then $\psi = 3$ mrad and $1/\gamma_0 = 0.5$ mrad, which agree with the divergence angle in parallel $[\theta \sim (-3.2, 0)$ mrad] and perpendicular $[\phi \sim (-0.7, 0.7)$ mrad] directions (Figs. 3 and 4), respectively. The expression for K is $(e/2mc^2)(x_1 + x_2)E_m \cot\alpha$. In our case, K is about 6; thus, radiation is more similar to from a wiggler. Therefore, we can adopt a similar analysis as in the wiggler. For example, the trajectory of a TNSF-kick electron can be considered as K decoupled sections, and each section can be approximated by an instantaneous circular motion. A critical frequency can then be determined based on the minimal radius of curvature of the trajectory $\rho_{min} = (mc^2\gamma)/(eE_m \cos\alpha)$. Therefore, we have $\omega_c = (3/2)(e/mc)(\gamma^2 E_m \cos\alpha)$. By changing the parameter γ_0, the spectra for electrons of different energies are presented in Fig. 5, which shows that the incident angle and TNSF parameters are the same as in Fig. 3. The critical frequency for the different electron energies shown in a black dashed line provides the frequency at which the radiation intensity drops to approximately half of the maximum. The radiation energy below the critical frequency is approximately 60% of the total radiation energy.

III. RADIATION OF ELECTRON BEAM

In the experiment, an electron beam instead of a single electron is used to produce bright X-ray radiation. For example, the spectrum of an electron beam with the following parameters is calculated. The total electron number is 2×10^9(i.e., 320 pC), which is uniformly distributed from 0.85 GeV to 1.15 GeV. For photon energy in the range of 0.1 MeV to 4 MeV, electrons of energy ranging from 0.2 GeV to 1.4 GeV have a notable contribution according to the expression of critical frequency ω_c. The beam pulse duration is 10 fs, and the beam emittance is $\epsilon_i = \sigma_i\theta_i = 1.6 \times 10^{-3}$ mm mrad ($i = y, z$) (the normalized emittance remains π mm mrad for beams of different energies). These electron beam parameters are reasonable for the current LPAs. To calculate the radiation brightness, we can estimate the

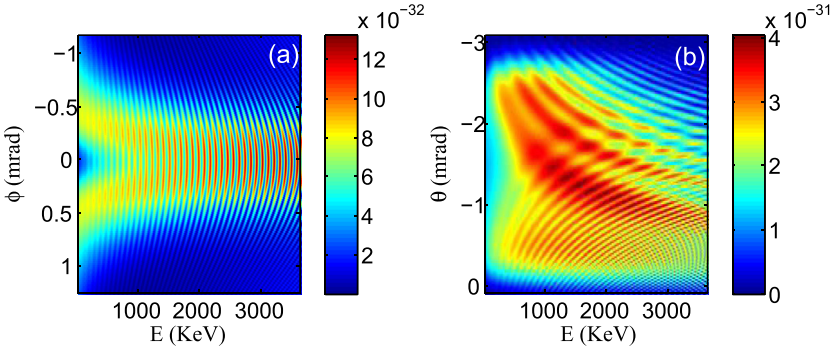

FIG. 3. Spectra in perpendicular (a) and parallel (b) plane $dI/d\omega d\Omega$ (J s rad sr^{-1}) for TNSF kick.

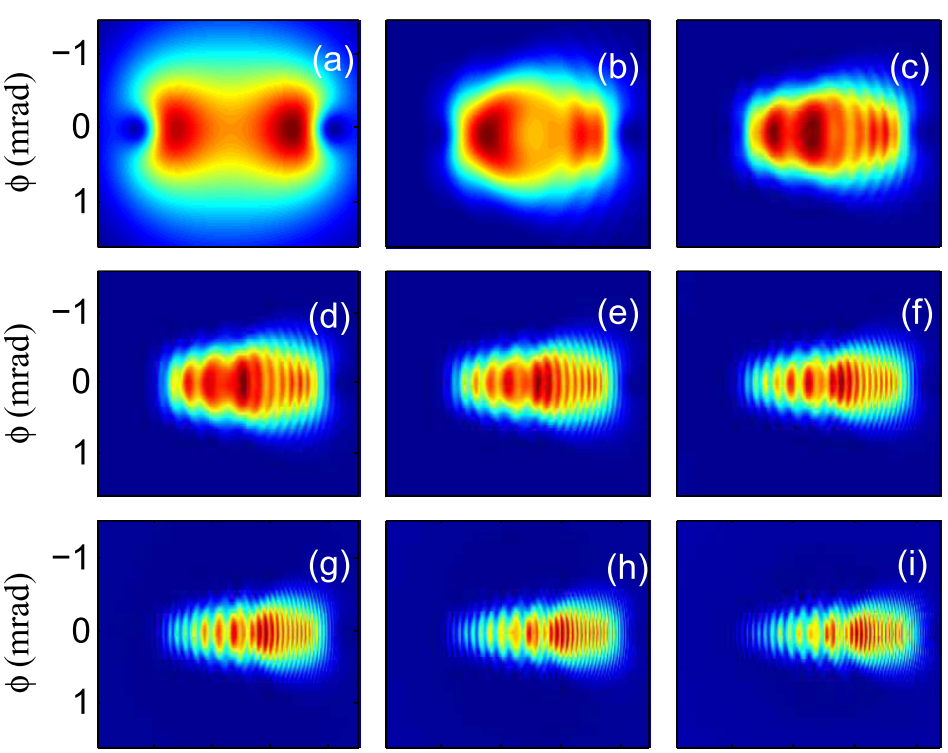

FIG. 4. Solid angle distribution of photons with different photon energies for TNSF kick. The electron energy is 1 GeV, and the incidence angle is $\alpha = \pi/18$. The photon energies from (a) to (i) are 0.066, 0.40, 0.72, 1.05, 1.38, 1.71, 2.04, 2.37, and 2.70 MeV.

divergence angle of the radiated X-ray beam as $\theta_{\mathrm{xbeam,i}} = (\theta^2_{\mathrm{ebeam,i}} + \theta^2_{\mathrm{espec,i}})^{1/2} (i = y, z)$,[24] where $\theta_{\mathrm{ebeam,i}}$ and $\theta_{\mathrm{espec,i}}$ are the divergence angles of the electron beam and spectra of a single electron, respectively. We assume the previously mentioned beam (beam emittance of 1.6×10^{-3} mm mrad) has a divergence angle $\theta_{\mathrm{ebeam,z}} = \theta_{\mathrm{ebeam,y}} = 1.6$ mrad and transverse size $\sigma_{\mathrm{ebeam,z}} = \sigma_{\mathrm{ebeam,y}} = 1.0\,\mu$m.[13] In this approach, the transverse size of the X-ray beam is the same as that of the electron beam, $\sigma_{\mathrm{xbeam,i}} = \sigma_{\mathrm{ebeam,i}}$ $(i = y, z)$. The radiation angles are calculated to be $\theta_{\mathrm{xbeam,z}} = 2.3$ mrad and $\theta_{\mathrm{xbeam,y}} = 1.7$ mrad, which are used below for the integration solid angle. A beam transport system is needed between the LPA and foil, and it may limit the beam brightness due to the growth of emittance.[26] By putting the foil in the gas of LPA, the problem of beam transport may be avoided. But it may lead other problems. Fig. 6 shows the spectrum of an electron beam. In our TNSF kick case, the spectrum is quite broad and very slowly decreases for a higher photon energy compared with the synchrotron spectra.[7] These characteristics are mainly due to the intrinsic broad spectrum of the single electron in the TNSF-kick scheme. As shown in Fig. 5, the spectrum of a single electron with different energies has almost the same start frequency but different peak and critical frequencies. Consequently, an electron beam with a large energy spread provides an X-ray beam with a spectrum band, whereas the critical frequency can be decided approximately by the average energy of the electron beam. The radiation spectrum of the electron beam appears similar to the case of a single electron, but with a higher intensity because

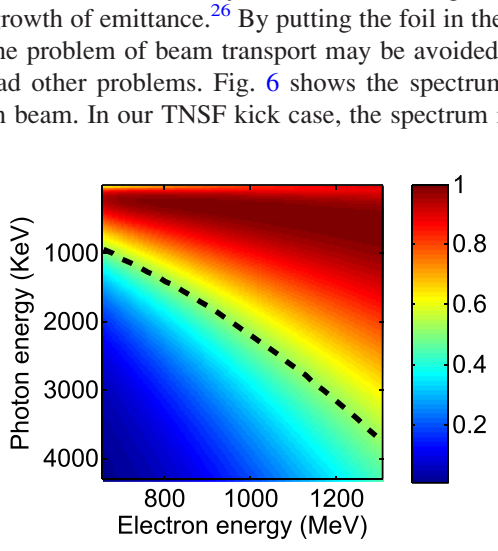

FIG. 5. Spectra for different electron energies. The black dashed line denotes the analytical critical frequency $\omega_c = (3/2)(e/mc)(\gamma^2 E_m \cos\alpha)$.

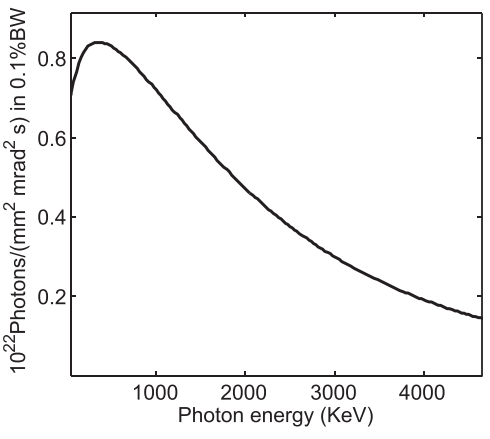

FIG. 6. Radiation spectrum of an electron beam for the TNSF-kick scheme integrated over a solid angle $\theta \sim (-4.6, 0)$ mrad, $\phi \sim (-1.7, 1.7)$ mrad for the beam of energy from 0.85 GeV to 1.15 GeV. The total electron number is 2×10^9 (i.e., 320 pC), the beam pulse length is 10 fs, and the beam emittance is $\epsilon_i = \sigma_i \theta_i = 1.6 \times 10^{-3}$ mm mrad $(i = y, z)$ (the normalized emittance remains at π mm mrad for the different beam energies).

of the accumulation effect of many electrons. The total number of X-ray photons (from 0.1 MeV to 4 MeV) is approximately 10^8, which contains approximately 80% of the total radiation energy, and the peak brightness is approximately 10^{22} photons/(s mm^2 mrad^2 0.1\%BW). This high peak brightness is mainly due to the small divergences in the single electron's spectrum in the TNSF kick and to the small emittance of the high-energy electron beam.

We now discuss how to obtain the same high brightness broadband radiation of photons around 1 MeV with other schemes. To obtain photons of MeV energy with an undulator, the energy required to drive an electron beam should be as high as 15 GeV,[1] which is much higher than what current LPAs can provide.[12] Using 15 GeV from conventional accelerators, the proposed TESLA spontaneous undulator can provide a narrow-bandwidth gamma-ray (0.1 MeV to 1 MeV) light with peak brilliance as high as 10^{26} photons/(s mm^2 mrad^2 0.1\%BW).[1] However, conventional accelerators for such high energy can be very huge and costly. For photons of energy higher than 1 MeV, another new concept of crystal undulator is proposed.[27] Here, we choose to calculate the radiation spectra of more promising Compton backscattering from an electron beam for comparison. We consider the following parameters. The laser pulse is of wavelength 810 nm, duration (FWHM) 15 fs, and peak normalized amplitude of the vector potential $a = 1.2$. To obtain a broadband X-ray with similar spectra as in the TNSF-kick scheme, we maintain the total electron number, pulse duration, and normalized emittance constant, but the energy spread from 0.1 to 0.4 GeV (chosen according the double Doppler shift formula to obtain photons from 0.1 MeV to 4 MeV). It is shown that the total number of X-ray photons (from 0.1 MeV to 4 MeV) is approximately 2×10^8 and the peak brightness is approximately 10^{20} photons/(s mm^2 mrad^2 0.1\%BW). Therefore, the Compton backscattering produces more photons, but the TNSF-kick radiation beam has a peak brightness about two orders higher because of the smaller transverse phase space area. On the other hand, betatron radiation in the bubble can also produce broadband radiation with brightness of 10^{23} photons/(s mm^2 mrad^2 0.1\%BW) in spectra between 20 and 150 KeV.[7] The radiation can be expanded to multi-MeV photons by using higher energy beams.

IV. DISCUSSION

In summary, we proposed a new scheme to get a broadband fs X-ray pulse source, fully utilizing the advantages of high energy and low emittance of LPA beams and its compactness. The drawbacks of the large energy spread of an LPA electron beam can be avoided. By using an electron beam with moderate charge (320 pC), high energy (expanding from 0.85 GeV to 1.15 GeV), ultrashort duration (10 fs), and low normalized emittance (πmm mrad), the TNSF kick approach can produce a 10 fs X-ray pulse with a broadband spectrum extending from 0.1 MeV to 4 MeV and peak brightness of about 10^{22} photons/(s mm^2 mrad^2 0.1\%BW). Therefore, the TNSF-kick source with a broadband fs hard X-ray pulse can serve as an alternative to costly and huge synchrotron X-ray sources. According to the formula $\omega_c \propto \gamma^2$, it is possible to obtain a high-brightness broadband gamma-ray of several tens MeV by using a more energetic beam (e.g., 2 GeV), with potential applications in nuclear physics such as nuclear resonance fluorescence experiments and pair production.

ACKNOWLEDGMENTS

This work has been supported by the Ministry of Science and Technology (2011CB808104 973, 2011DFA11300), National Natural Science Foundation of China (Projects No. 11125526, No. 11335013, No. 11374319, No. 11374317, No. 61008010, No. 11127901, and No. 60921004).

[1]See http://tesla.desy.de/new_pages/TDR_CD/PartV/fel.html for information about X-ray applications and radiation facilities.
[2]J. Drenth, *Principles of Protein X-Ray Crystallography* (Springer-Verlag GmbH, New York, 1999).
[3]A. Rousse, C. Rischel, and J.-C. Gauthier, Rev. Mod. Phys. **73**, 17 (2001).
[4]B. C. Larson, W. Yang, G. E. Ice, J. D. Budai, and J. Z. Tischler, Nature (London) **415**, 887 (2002).
[5]R. Smith and M. H. Key, J. Phys. IV France **11**, Pr2-383 (2001).
[6]S. Chen, N. D. Powers, I. Ghebregziabher, C. M. Maharjan, C. Liu, G. Golovin, S. Banerjee, J. Zhang, N. Cunningham, A. Moorti, S. Clarke, S. Pozzi, and D. P. Umstadter, Phys. Rev. Lett. **110**, 155003 (2013).
[7]S. Cipiccia, M. R. Islam, B. Ersfeld, R. P. Shanks, E. Brunetti, G. Vieux, X. Yang, R. C. Issac, S. M. Wiggins, G. H. Welsh, M.-P. Anania, D. Maneuski, R. Montgomery, G. Smith, M. Hoek, D. J. Hamilton, N. R. C. Lemos, D. Symes, P. P. Rajeev, V. O. Shea, J. M. Dias, and D. A. Jaroszynski, Nat. Phys. **7**, 867 (2011).
[8]A. Macchi, M. Borghesi, and M. Passoni, Rev. Mod. Phys. **85**, 751 (2013).
[9]W. P. Wang, H. Zhang, B. Wu, C. Y. Jiao, Y. C. Wu, B. Zhu, K. G. Dong, W. Hong, Y. Q. Gu, B. F. Shen, Y. Xu, Y. X. Leng, R. X. Li, and Z. Z. Xu, Appl. Phys. Lett. **101**, 214103 (2012).
[10]F. V. Hartemann, D. J. Gibson, W. J. Brown, A. Rousse, K. T. Phuoc, V. Mallka, J. Faure, and A. Pukhov, Phys. Rev. ST Accel. Beams **10**, 011301 (2007).
[11]R. Maaß, S. Van Petegem, H. Van Swygenhoven, P. M. Derlet, C. A. Volkert, and D. Grolimund, Phys. Rev. Lett. **99**, 145505 (2007).
[12]X. Wang, R. Zgadzaj, N. Fazel, Z. Li, S. A. Yi, X. Zhang, W. Henderson, Y. Y. Chang, R. Korzekwa, H. E. Tsai, C. H. Pai, H. Quevedo, G. Dyer, E. Gaul, M. Martinez, A. C. Bernstein, T. Borger, M. Spinks, M. Donovan, V. Khudik, G. Shvets, T. Ditmire, and M. C. Downer, Nat. Commun. **4**, 1988 (2013).
[13]E. Esarey, C. B. Schroeder, and W. P. Leemans, Rev. Mod. Phys. **81**, 1229 (2009).
[14]K. T. Phuoc, S. Corde, C. Thaury, V. Malka, A. Tafzi, J. P. Goddet, R. C. Shah, S. Sebban, and A. Rousse, Nat. Photon. **6**, 308 (2012).
[15]M. Wen, L. Jin, Y. Lu, J. Chen, and X. Yan, Appl. Phys. Lett. **101**, 021102 (2012).
[16]M. Fuchs, R. Weingartner, A. Popp, Z. Major, S. Becker, J. Osterhoff, I. Cortrie, B. Zeitler, R. Horlein, G. D. Tsakiris, U. Schramm, T. P. Rowlands-Rees, S. M. Hooker, D. Habs, F. Krausz, S. Karsch, and F. Gruner, Nat. Phys. **5**, 826 (2009).
[17]H.-P. Schlenvoigt, K. Haupt, A. Debus, F. Budde, O. Jackel, S. Pfotenhauer, H. Schwoerer, E. Rohwer, J. G. Gallacher, E. Brunetti, R. P. Shanks, S. M. Wiggins, and D. A. Jaroszynski, Nat. Phys. **4**, 130 (2008).
[18]S. Kneip, C. McGuffey, J. L. Martins, S. F. Martins, C. Bellei, V. Chvykov, F. Dollar, R. Fonseca, C. Huntington, G. Kalintchenko, A. Maksimchuk, S. P. D. Mangles, T. Matsuoka, S. R. Nagel, C. A. J. Palmer, J. Schreiber, K. T. Phuoc, A. G. R. Thomas, V. Yanovsky, L. O. Silva, K. Krushelnick, and Z. Najmudin, Nat. Phys. **6**, 980 (2010).
[19]Z. Huang, Y. Ding, and C. B. Schroeder, Phys. Rev. Lett. **109**, 204801 (2012).
[20]S. Cipiccia, S. M. Wiggins, R. P. Shanks, M. R. Islam, G. Vieux, R. C. Issac, E. Brunetti, B. Ersfeld, G. H. Welsh, M. P. Anania, D. Maneuski, N. R. C. Lemos, R. A. Bendoyro, P. P. Rajeev, P. Foster, N. Bourgeois, T. P.

A. Ibbotson, P. A. Walker, V. O. Shea, J. M. Dias, and D. A. Jaroszynski, J. Appl. Phys. **111**, 063302 (2012).
[21]M. Chen, E. Esarey, C. G. R. Geddes, C. B. Schroeder, G. R. Plateau, S. S. Bulanov, S. Rykovanov, and W. P. Leemans, Phys. Rev. ST Accel. Beams **16**, 030701 (2013).
[22]J. D. Jackson, *Classical Electrodynamics*, 3rd ed. (Wiley, New York, 1999).
[23]A. G. R. Thomas, Phys. Rev. ST Accel. Beams **13**, 020702 (2010).
[24]E. Esarey, S. K. Ride, and P. Sprangle, Phys. Rev. E **48**, 3003 (1993).
[25]S. Corde, K. Ta Phuoc, G. Lambert, R. Fitour, V. Malka, A. Rousse, A. Beck, and E. Lefebvre, Rev. Mod. Phys. **85**, 1 (2013).
[26]M. Migliorati, A. Bacci, C. Benedetti, E. Chiadroni, M. Ferrario, A. Mostacci, L. Palumbo, A. R. Rossi, L. Serafini, and P. Antici, Phys. Rev. ST Accel. Beams **16**, 011302 (2013).
[27]See http://ec.europa.eu/research/fp6/nest/pdf/whats_next/pecu.pdf for information about crystal undulator.